

## Room Temperature Bis-tolane Liquid Crystals

This content has been downloaded from IOPscience. Please scroll down to see the full text.

1999 Jpn. J. Appl. Phys. 38 L286

(<http://iopscience.iop.org/1347-4065/38/3B/L286>)

View [the table of contents for this issue](#), or go to the [journal homepage](#) for more

Download details:

IP Address: 140.113.38.11

This content was downloaded on 28/04/2014 at 10:40

Please note that [terms and conditions apply](#).

## Room Temperature Bis-tolane Liquid Crystals

Shin-Tson WU, Chain-Shu HSU<sup>1</sup> and Ya-Yuen CHUANG<sup>1</sup>

HRL Laboratories, 3011 Malibu Canyon Road, Malibu, CA 90265, U.S.A.

<sup>1</sup>Department of Applied Chemistry, National Chiao Tung University, Hsinchu, Taiwan 30050, Republic of China

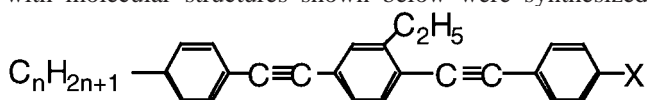
(Received February 5, 1999; accepted for publication February 12, 1999)

Several room temperature bis-tolane liquid crystals were synthesized and their physical properties evaluated at elevated temperatures. These highly conjugated liquid crystals exhibit not only high birefringence ( $\Delta n > 0.4$ ) but also low melting temperature. Their applications for flat panel displays employing light scattering or Bragg reflection and for infrared spatial light modulators are emphasized.

KEYWORDS: bis-tolane liquid crystal, high birefringence, wide nematic range

High birefringence ( $\Delta n$ ) liquid crystals (LCs) are particularly attractive for reflective displays involving cholesterics<sup>1)</sup> and polymer-dispersed LC,<sup>2)</sup> laser beam steering employing optical phased arrays<sup>3)</sup> and infrared spatial light modulators for non-destructive missile seeker simulations.<sup>4)</sup> For a cholesteric display using Bragg reflection, high  $\Delta n$  widens the reflection spectral bandwidth and improves the display brightness. For polymer-dispersed LC, high  $\Delta n$  would enhance light scattering efficiency and contrast ratio. For LC-based optical phased arrays and infrared spatial light modulators, high  $\Delta n$  helps to shorten response time through thinner cell gap requirement. Based on the single-band<sup>5)</sup> and three-band<sup>6)</sup> birefringence dispersion models, the LC birefringence is mainly determined by the molecular conjugation, differential oscillator strength and order parameter. Thus, a more linearly conjugated rod-like LC would exhibit a larger optical anisotropy. A general problem of these highly conjugated molecules is that their melting temperature is usually quite high. From Schroder-Van Laar equation,<sup>7,8)</sup> a LC compound with high melting point ( $T_{mp}$ ) and large heat fusion enthalpy ( $\Delta H$ ) would result in a poor solubility while forming eutectic mixtures.

In this paper, we report a new series of high birefringence bis-tolane liquid crystals. In addition to high birefringence, these highly conjugated LCs possess a surprisingly low melting temperature and wide nematic range. More than 10 dialkyl and polar (cyano and fluoro) bis-tolanes with molecular structures shown below were synthesized:



where  $X = C_mH_{2m+1}$ , F or CN. For simplicity, these alkyl-alkyl, fluoro and cyano bis-tolane LCs are abbreviated as PTP(3-Et)TP-nm, PTP(3-Et)TP-nF and PTP(3-Et)TP-nCN, respectively; here P stands for the phenyl ring, T for the carbon-carbon triple bond, and P(3-Et) for the middle phenyl ring with an ethyl group sticking out at the 3-position.

The phase transition temperatures, heat fusion enthalpy and dielectric anisotropy of the bis-tolanes we synthesized are listed in Table I. Some similar compounds but with different substituents (methyl or hydrogen group)<sup>9)</sup> in the middle phenyl ring are also included for comparison. From Table I, we find that the bis-tolanes we studied exhibit a wide nematic range and small heat fusion enthalpy. More surprisingly, some bis-tolanes (-52, -53, -62 and -63) remain liquid at room temperature. We had to cool the samples to  $-170^\circ\text{C}$  and run differential scanning calorimeter very slowly (at  $1^\circ\text{C}/\text{min}$ ) in

order to resolve the melting point. In the cooling process, the solidification temperature was found to be below  $-50^\circ\text{C}$ .

The middle ethyl group plays a key role to the observed low melting temperature. From Table I, PTP(3-Et)TP-52, 62 and 63 exhibit a much lower melting temperature than their methyl and hydrogen counterparts. This is because the ethyl group extends the molecular breadth and then loosens the inter-molecular packing density. As a result, the required temperatures to melt and to clear the LC clusters are both lower. Continue to increase the length of such alkyl substituent will further decrease the melting point, however, its viscosity will substantially increase.

To characterize the birefringence dispersion of these new bis-tolanes, we have selected PTP(3-Et)TP-53 for studies at room temperature ( $T = 22^\circ\text{C}$ ) which corresponds to a reduced temperature of  $T_r = 0.743$ ; here  $T_r$  is defined as  $T/T_c$ ;  $T_c$  being the clearing temperature. A homogeneous cell with  $d = 4.8\text{-}\mu\text{m}$  was used for measuring  $\Delta n$  through phase retardation determination ( $\delta = 2\pi d\Delta n/\lambda$ ).<sup>10)</sup> Three light sources were used for such measurements: a computer controlled Perkin-Elmer Lambda-9 spectrophotometer, an argon-ion ( $\lambda = 488$  and  $514.5$  nm) laser and a HeNe ( $\lambda = 633$  nm) laser. Results are depicted in Fig. 1. Here the open circles represent experimental data measured from spectrophotometer, filled circles are from lasers, and the solid lines are fittings using the single-band model:<sup>5)</sup>

$$\Delta n = G \frac{\lambda^2 \lambda^{*2}}{\lambda^2 - \lambda^{*2}} \quad (1)$$

In eq. (1), parameter  $G$  is a proportionality constant and  $\lambda^*$  is the mean electronic transition wavelength. The order parameter ( $S$ ) that governs the temperature dependency of  $\Delta n$  is included in  $G$ . From fittings,  $G$  and  $\lambda^*$  are found to be  $3.33 \mu\text{m}^{-2}$  and  $\lambda^* = 0.292 \mu\text{m}$ , respectively. From Fig. 1, the birefringence of PTP(3-Et)TP-53 exceeds 0.4 in the blue and green regions. As the wavelength increases,  $\Delta n$  decreases gradually and saturates in the near infrared region.

Besides birefringence, viscosity and dielectric anisotropy are also important for display and electro-optic applications. To measure the temperature-dependent birefringence and visco-elastic coefficient ( $\gamma_1/K_{11}$ ), we prepared a homogeneous cell and measured its voltage-dependent phase retardation and transient phase decay time.<sup>10)</sup> A HeNe laser was used for these measurements. The indium-tin-oxide coated glass substrates were evaporated with  $\text{SiO}_x$  layers to produce uniform homogeneous LC alignment with pretilt angle of  $\sim 2^\circ$ . The cell gap was controlled to be  $d = 7.6 \mu\text{m}$ .

Table I. Phase transition temperatures (in °C), heat fusion enthalpy ( $\Delta H$ , in kcal/mol), and dielectric anisotropy ( $\Delta\epsilon$ ) of the dialkyl, fluoro and cyano bis-tolane liquid crystals. Also included for comparisons are homologues with a methyl (\*) and hydrogen (\*\*) substituents, instead of ethyl group in the middle phenyl group.

PTP(3-Et)TP-	$T_{mp}$	$T_c$	$\Delta H$	$\Delta\epsilon$
23	73.9	141.5	3.34	
25	58.4	124.6	2.85	
32	55.5	141.0	3.45	
35	56.1	134.9	2.99	
36	56.9	120.4	3.04	
52	29.4	120.0	3.25	
52*	61.6	173.5	3.54	
53	25.7	124.0	4.70	0.85
62	31.0	106.8	3.18	
62*	61.0	168.7	5.80	
62**	133.6	191.1	3.61	
63	20.0	107.8	3.50	
63*	51.3	168.7	3.28	
5F	60.9	103.2	5.54	
5CN	85.2	159.3	5.88	~14

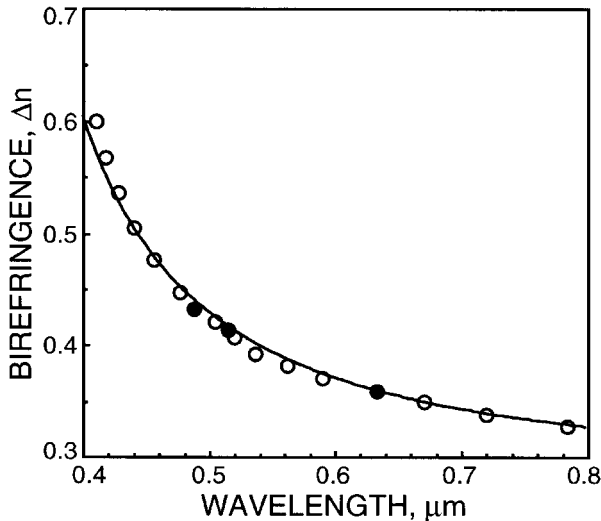


Fig. 1. The wavelength-dependent birefringence of PTP(3-Et)TP-53 at  $T = 22^\circ\text{C}$ . Open circles are data measured from spectrophotometer, filled circles are data from  $\text{Ar}^+$  and HeNe laser lines, and solid lines are fittings using eq. (1) with  $G = 3.33 \mu\text{m}^{-2}$  and  $\lambda^* = 0.292 \mu\text{m}$ .

The temperature-dependent birefringence (open circles) and visco-elastic coefficient (squares) of PTP(3-Et)TP-53 are shown in the right and left hand-side of Fig. 2, respectively. The solid lines for the birefringence represent fittings using the following equations:

$$\Delta n = (\Delta n)_0 S \quad (2)$$

$$S = [1 - T_r]^\beta \quad (3)$$

In eq. (2),  $\Delta n_0$  stands for the birefringence as order parameter  $S = 1$  (a perfect crystalline state), and beta is a material parameter. Equation (3) is Haller's approximation<sup>11)</sup> for order parameter. This approximation holds reasonably well in the range that  $T_c - T > 2$  degrees. Fitting experimental data with eqs. (2) and (3), we obtain  $\Delta n_0 = 0.484$  at  $\lambda = 633 \text{ nm}$  and  $\beta = 0.219$ . From eq. (1),  $\Delta n_0$  decreases as wavelength increases. By contrast,  $\beta$  is only dependent on the LC structure

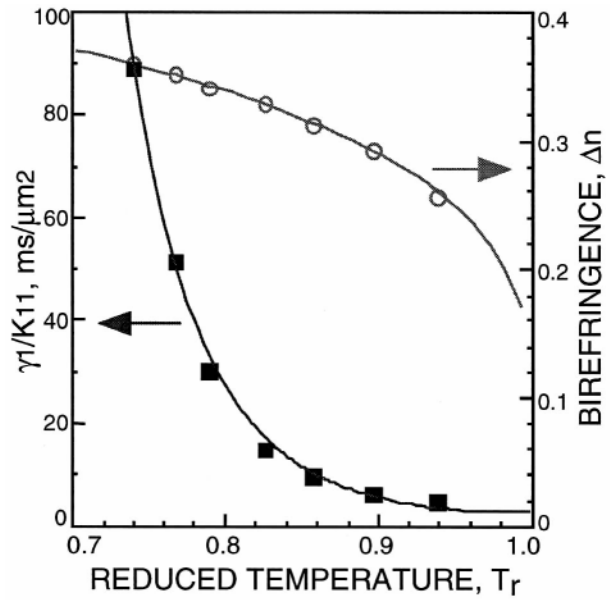


Fig. 2. The temperature-dependent birefringence (circles) and visco-elastic coefficient (squares). Solid lines for  $\Delta n$  are fittings using eqs. (2) and (3) with  $\Delta n_0 = 0.484$  and  $\beta = 0.219$ , and for  $\gamma_1/K_{11}$  are fittings using eq. (6) with  $A = 3.37 \times 10^{-6} \text{ ms}/\mu\text{m}^2$  and  $E = 0.429 \text{ eV}$ .  $\lambda = 633 \text{ nm}$ .

and independent of wavelength.

The temperature-dependent rotational viscosity ( $\gamma_1$ ) and splay elastic constant ( $K_{11}$ ) can be described by the following equations:<sup>12,13)</sup>

$$\gamma_1 \sim S \exp(E/kT) \quad (4)$$

$$K_{11} \sim S^2 \quad (5)$$

where  $E$  is the activation energy and  $k$  is the Boltzmann constant. Combining eqs. (3)–(5), the visco-elastic coefficient has the following expression:

$$\gamma_1/K_{11} = A \exp(E/kT)/[1 - T_r]^\beta \quad (6)$$

In Fig. 2, squares represent measured data on the visco-elastic coefficient of PTP(3-Et)TP-53 and solid lines are fittings using eq. (6). From the fittings, we found the proportionality constant  $A = 3.37 \times 10^{-6} \text{ ms}/\mu\text{m}^2$  and activation energy  $E = 0.429 \text{ eV}$ . The relatively high activation energy hinders the LC clusters from moving freely and, thus, increases the rotational viscosity.

As the temperature increases, both birefringence, viscosity and elastic constant decrease. However, at a temperature that is far away from  $T_c$ , the decreasing rate of visco-elastic coefficient is faster than birefringence. This is due to the exponential temperature dependence of rotational viscosity, as described in eq. (4). When  $T_r > 0.85$ , the situation is reversed. Although the viscosity continues to decline as temperature increases, the elastic constant also decreases sharply. As a result, the decreasing rate of birefringence surpasses that of visco-elastic coefficient. Thus, there exists an optimal operation temperature where the maximum figure-of-merit (defined as  $K_{11} \Delta n^2/\gamma_1$ ) occurs.<sup>14)</sup> This figure-of-merit takes the phase change and response time of a LC phase modulator into account and is an important parameter for optimization.

The dielectric anisotropy ( $\Delta\epsilon$ ) affects the threshold voltage ( $V_{th}$ ) of a LC device. For example, the threshold voltage of a

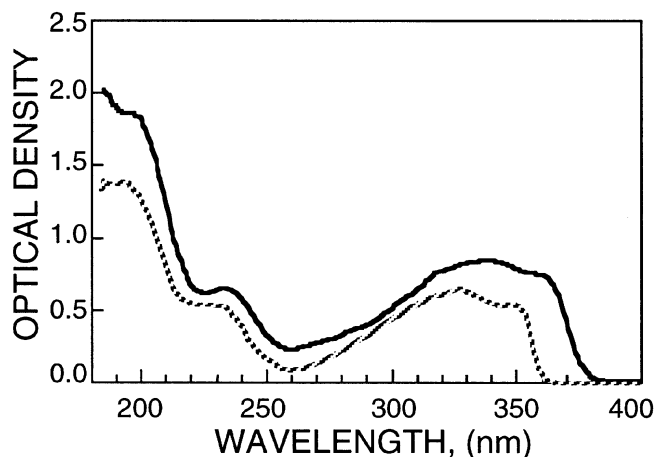


Fig. 3. The absorption spectra of PTP(3-Et)TP-5CN (solid lines) and PTP(3-Et)TP-53 (dashed lines). In experiment, 1% of each LC compound studied was dissolved in ZLI-2359. Cell gap  $d = 6 \mu\text{m}$ .  $T_r = 0.865$ .

homogeneous cell is related to dielectric anisotropy and splay elastic constant as:<sup>15)</sup>

$$V_{\text{th}} = \pi \sqrt{K_{11}/\varepsilon_0 \Delta\varepsilon}. \quad (7)$$

From mean-field theory,<sup>16)</sup>  $\Delta\varepsilon$  is determined by the dipole moment and its orientation angle with respect to the principal molecular axis. The dialkyl bis-tolane we synthesized is non-polar. Thus, its  $\Delta\varepsilon$  is expected to be small. To measure dielectric constants, we used the capacitance method.<sup>10)</sup> A LC cell with patterned electrode was used. A HP-4274A Multi-Frequency LCR Meter was used for capacitance measurements. The measured dielectric constants for PTP(3-Et)TP-53 are  $\Delta\varepsilon_{//} = 3.37$  and  $\varepsilon_{\perp} = 2.52$  at 1 kHz sine-wave frequency and  $T = 22^{\circ}\text{C}$ . Also, from the measured threshold voltage  $V_{\text{th}} = 3.82 V_{\text{rms}}$ , the splay elastic constant is found to be  $K_{11} \sim 11.0 \text{ pN}$ .

We have also measured the dielectric anisotropy and birefringence of PTP(3-Et)TP-5CN. Owing to the high melting point of this compound, we measured its  $\Delta\varepsilon$  and  $\Delta n$  using the guest-host method<sup>10)</sup> in which we mixed 10% PTP(3-Et)TP-5CN in the PTP(3-Et)TP-53 host. The extrapolated  $\Delta\varepsilon$  of PTP(3-Et)TP-5CN is 14 at  $T = 22^{\circ}\text{C}$  and  $\Delta n$  is 0.42, 0.46 and 0.50 for  $\lambda = 633, 514.5$  and  $488 \text{ nm}$ , respectively. The exceedingly high birefringence of PTP(3-Et)TP-5CN results from its long molecular conjugation. The cyano group not only possesses a large dipole, but also causes a noticeable red shift in absorption wavelength, as shown in Fig. 3.

Figure 3 compares the absorption spectra of PTP(3-Et)TP-5CN to PTP(3-Et)TP-53. Normally, the electronic absorption of conjugated molecules are quite strong in the ultraviolet region.<sup>17)</sup> In order to obtain a sufficient signal-to-noise ratio, in experiment we only dissolved 1% of each compound studied in an UV transparent LC mixture ZLI-2359 (from Merck). A homogeneous cell with  $6 \mu\text{m}$  gap and quartz substrates was used for the absorption measurements. Thus, the indicated optical density in Fig. 3 is equivalent to a  $0.06\text{-}\mu\text{m}$  thick pure LC substance. From Fig. 3, the red shift caused by the cyano group is about 20 nm. Based on eq. (1), a longer  $\lambda^*$  would lead to a higher birefringence. A general drawback of the cyano compound is its large viscosity. By adding 10% of PTP(3-Et)TP-5CN to PTP(3-Et)TP-53, the mixture's visco-elastic coefficient is increased by  $\sim 15\%$  at  $T = 22^{\circ}\text{C}$ , as compares to the PTP(3-Et)TP-53 host alone.

In conclusion, we have synthesized several bis-tolane LC compounds that possess high birefringence, low melting and high clearing temperatures, and small heat of fusion enthalpy. These compounds will find useful applications in reflective displays employing cholesteric liquid crystals, laser beam steering employing liquid crystal optical phased arrays and infrared spatial light modulators for non-destructive missile seeker testing.

The HRL group is indebted to W. H. Smith, Jr. for the technical assistance.

- 1) D. K. Yang, J. W. Doane, Z. Yaniv and J. Glasser: *Appl. Phys. Lett.* **64** (1994) 1905.
- 2) J. L. Ferguson: *SID Tech. Dig.* **16** (1985) 68.
- 3) P. F. McManamon, E. A. Watson, T. A. Dorschner and L. J. Barnes: *Opt. Eng.* **32** (1993) 2657.
- 4) S. T. Wu, U. Efron, J. Grinberg and L. D. Hess: *SID Tech. Dig.* **16** (1985) 262.
- 5) S. T. Wu: *Phys. Rev. A* **30** (1986) 1270.
- 6) S. T. Wu, C. S. Wu, M. Warengem and M. Ismaili: *Opt. Eng.* **32** (1993) 1775.
- 7) L. Schroder: *Z. Phys. Chem.* **11** (1893) 449.
- 8) J. J. Van Laar: *Z. Phys. Chem.* **63** (1908) 216.
- 9) S. T. Wu, C. S. Hsu and K. F. Shyu: *Appl. Phys. Lett.* **74** (1999) 344.
- 10) I. C. Khoo and S. T. Wu: *Optics and Nonlinear Optics of Liquid Crystals* (World Scientific, Singapore, 1993).
- 11) I. Haller: *Prog. Solid State Chem.* **10** (1975) 103.
- 12) V. V. Belyaev, S. A. Ivanov and M. F. Gorebenkin: *Sov. Phys. Crystallogr.* **30** (1985) 674.
- 13) A. Saupe: *Z. Naturforsch. Teil A* **15** (1960) 810.
- 14) S. T. Wu, A. M. Lackner and U. Efron: *Appl. Opt.* **26** (1987) 3441.
- 15) H. J. Deuling: *Elasticity of Nematic Liquid Crystals, Solid State Phys. Suppl. 14: Liquid Crystals*, ed. L. Liebert (Academic, New York, 1978).
- 16) W. Maier and G. Meier: *Z. Naturforsch. Teil A* **16** (1961) 262.
- 17) S. T. Wu, E. Ramos and U. Finkenzeller: *J. Appl. Phys.* **68** (1990) 78.